

Optical transitions between light hole subbands in InGaAs/InP strained layer multiquantum wells

I. Ilouz, J. Oiknine-Schlesinger, D. Gershoni, and E. Ehrenfreund

Department of Physics and Solid State Institute, Technion-Israel Institute of Technology, Haifa 32000, Israel

D. Ritter

Department of Electrical Engineering and Solid State Institute, Technion-Israel Institute of Technology, Haifa 32000, Israel

R. A. Hamm and J. M. Vandenberg

AT&T Bell Laboratories, Murray Hill, New Jersey 07974

(Received 24 October 1994; accepted for publication 2 February 1995)

The observation of light hole intersubband absorption in both *p*-doped and photoexcited undoped strained In_xGa_{1-x}As/InP (*x*≈0.35) quantum-well structures is reported. The absorption is polarized along the growth direction and is in agreement with calculations which show that the strain causes the light hole level to be first occupied upon *p*-doping or photoexcitation. Both impurity bound and free holes transitions are identified. © 1995 American Institute of Physics.

Strained layer superlattices (SLSs) are of considerable interest due to the added flexibility in controlling their optical and electrical transport properties. The biaxial in-plane strain caused by lattice constant mismatch, profoundly affects the electronic band structure. For a tensively strained In_xGa_{1-x}As/InP (*x*<0.53) layer, for instance, the light hole (*m_J*=1/2, lh) valence band edge is above the heavy hole (*m_J*=3/2, hh) edge.¹ Thus, in tensile SLSs the uniaxial strain is opposite in sign to the quantum size effect. As a result, a strained quantum well (QW) system can be fabricated in which the first subvalence-level to be occupied is lh1, and the character of the valence band excitation becomes similar to that of the conduction band, since the confinement masses are comparable.

In this letter, we report the first observation of light hole intersubband transitions in In_xGa_{1-x}As/InP (*x*≈0.35) SLSs. The transitions, observed in both *p*-doped and undoped samples, were all polarized along the growth direction (*z* axis). Using interband excitation, we have identified lh1–lh2 absorption of “free” photogenerated holes. Without interband excitation, we have observed blue shifted broader absorption lines. We interpret these lines, as optical transitions between two levels of a neutral acceptor. The acceptor levels are associated with the intrinsic lh1 and lh2 levels, respectively.

Three In_xGa_{1-x}As/InP samples were used in this study: a *p*-type doped strained MQW structure (sample I, *x*=0.36) a similar but nominally undoped strained structure (sample II, *x*=0.34) and a reference, *p*-type doped, and slightly compressively strained MQW structure (sample III, *x*=0.55). The samples were grown on a semi-insulating (100) oriented InP substrates, by metalorganic molecular beam epitaxy.² We used Be as the *p*-dopant which was introduced during growth to the center 6 nm of each ternary layer. The nominally undoped ternary layers were residually *n*-type with background concentration lower than ≈1×10¹⁶ cm⁻³. The layer widths and their compositions were accurately determined using high resolution x-ray diffraction. The dimensions, composi-

tions, and doping levels of the samples are given in Table I. For the absorption and photoinduced absorption (PIA) measurements the samples were fabricated as multipass waveguides by polishing two parallel cleaved facets at a 45° angle. In this way, the electric field of the *p*-polarized infrared (IR) beam, which propagates along the waveguide, has a component along the growth direction [see inset Fig. 1(a)]. In addition, a 300 nm thick gold layer was deposited on the *p*-doped samples on their waveguide side closest to the quantum structure, in order to enhance this component of the electric field.³

The optical measurements were done using a Bruker IFS66V FTIR spectrometer equipped with a step scan mirror movement to allow pump beam modulation using conventional lock-in techniques. The absorption results are given as $-\ln(T_p/T_s)$, where *T_s* (*T_p*) is the transmission through the sample for IR light polarized in the *s*(*p*) configurations [see insert Fig. 1(a)]. For the PIA studies the 1.06 μm line of a Nd:YAG laser was used for the excitation. The light was inserted through the uncoated substrate side of the multipass waveguide. The photoinduced change in the absorbance is given by $-\Delta T_p/T_p$, where Δ*T_p* is the photoinduced change of *T_p*.

In Fig. 1(a) we show by the solid line the absorption spectrum of the strained *p*-type doped sample (sample I). The dashed line in Fig. 1(a) represents a similar absorption spectrum of the nearly unstrained *p*-type doped sample (sample III). It is clearly seen that while the spectrum of sample I consists of an asymmetric band which peaks around 143 meV and has a full width at half maximum (FWHM) of ≈18 meV, the other spectrum is featureless. The observed band is polarized along the growth direction as might have been expected for optical transitions between discrete subbands of the same band. We, therefore, safely conclude that the observed band signifies an intersubband transition within the valence band manifold of the strained MQW structure. Based on our previous studies,⁴ we assign this transition to light

TABLE I. Samples parameters and transition energies for the $\text{In}_x\text{Ga}_{1-x}\text{As}/\text{InP}$ SLS reported here. The first four columns give the well width (d), barrier width (b), the number of periods and the InAs mole fraction (x). The fifth column gives the nominal p -doping density. The experimental PIA and absorption are given in the sixth and seventh columns, respectively (NO means not observed), and the calculated transition energies (lh1–lh2 for samples I and II, and $e1-e2$ for sample III) are given in the eighth one. The numbers in parenthesis represent the uncertainty in the last digit.

Sample	d (nm)	b (nm)	Periods	x	Doping (10^{11} cm^{-2})	PIA (meV)	Abs. (meV)	Cal. (meV)
I	7.2(3)	37.9(3)	10	0.36(1)	3	120(1)	143(1)	132(4)
II	9.8(3)	40.4(3)	15	0.34(1)	undoped	94(1)	NO	108(4)
III	6.1(3)	35.1(3)	10	0.55(2)	3	166(1)	NO	160(7)

holes. This assumption is further supported by our model calculations as follows.

Our calculations are carried out using an eight-band envelope function approximation $\mathbf{k}\cdot\mathbf{p}$ model, which accurately takes into account the lattice mismatch strain in the structure.⁵ The confined energy levels were identified by the number of nodes in their envelope wave functions and their total angular momentum projection on the QW symmetry axis at $k_{\parallel}=0$. It is found that the top of the first confined lh1 subband is ≈ 60 meV higher in energy than the top of the first confined hh1 level. This is expected for these biaxially tensile strained systems.¹ In Fig. 1(b) we display the calculated absorption spectrum of sample I, for the nominal hole

density of $3 \times 10^{11} \text{ cm}^{-2}$ per well and for $T=80$ K. The calculated spectrum consists of a distinct z -polarized spectral feature at 132 meV due to lh1–lh2 optical transition. A smaller feature at ≈ 60 meV (nearly unpolarized) is due to the lh1–hh1. The area under the calculated lh1–lh2 transition agrees within less than a factor of 2 with the measured one [Fig. 1(a)]. This is well within the uncertainty associated with the concentration of the Be dopants.

The PIA spectrum of sample I is displayed in Fig. 1(c) for p -polarized IR light. Like the absorption spectrum, the PIA spectrum consists of a single band, which is totally polarized along the growth direction. The band, however, has only ≈ 9 meV FWHM, and it peaks at 120 meV, 23 meV lower than the respective band observed in the absorption spectrum and ≈ 12 meV lower than the calculated band. The PIA spectrum of the undoped strained sample (sample II) is similar to that of sample I, and is shown in Fig. 2(a). The single band observed in this spectrum has FWHM of ≈ 6 meV and it peaks at 94 meV, ≈ 14 meV lower than the calculated lh1–lh2 transition for this sample which is displayed in Fig. 2(b). The PIA spectrum of sample III (not shown) is very similar to other spectra that we have observed in n -type unstrained InGaAs/InP MQW systems.⁶ It consists of only one band which is polarized along the growth direction, peaks around 166 meV and has FWHM of ≈ 9 meV. Like in the previously discussed spectra this band is assigned to intersubband absorption by photoexcited electrons which were added by the pump beam to the lowest conduction subband. Its energy and spectral shape are very close to the expected $e1-e2$ transition for this sample (see Table I). In the following, we discuss the transitions observed in the PIA spectra of the strained samples (samples I and II). We assign these transitions to intersubband absorption by photoexcited light holes added by the pump beam to the upper most valence subband of the strained quantum structure. Transitions between conduction subbands in these samples are expected at lower energies (less than ≈ 70 meV) due to the decrease in the potential depth of the conduction band QW in these low InAs mole fraction samples.⁷ We could not observe these long wavelength transitions with our present experimental setup, which is limited by the MCT detector spectral response. Moreover, similar to the unstrained intentionally undoped samples, sample II is also residually n -type doped. Yet, unlike the unstrained samples,⁶ it has no “dark” (i.e., in the absence of interband excitation) absorption line close in energy to the observed PIA line. This strongly indicates that

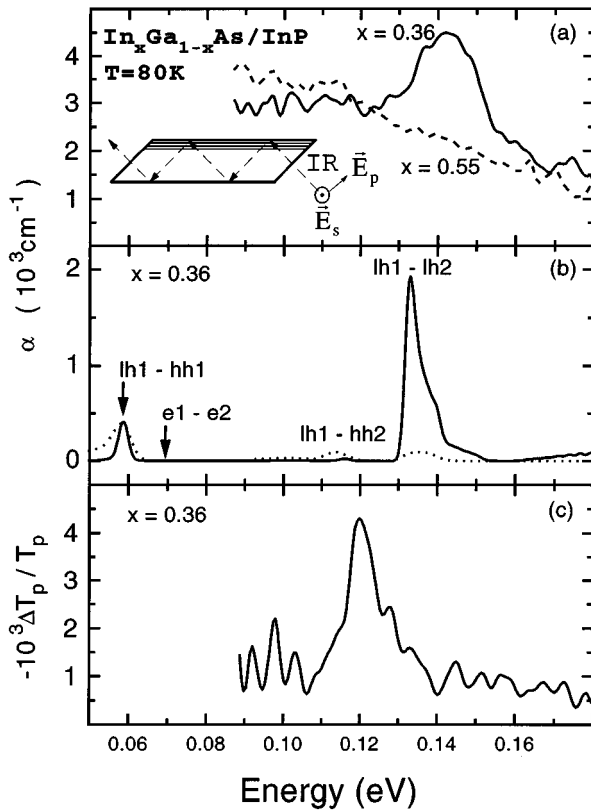


FIG. 1. (a) IR intersubband absorption coefficient, $\alpha \equiv -\ln(T_p/T_s)$, of the p -doped $\text{In}_x\text{Ga}_{1-x}\text{As}/\text{InP}$ samples. Solid line: sample I ($x=0.36$), dashed line: sample III ($x=0.55$). Inset: the waveguide configuration. (b) Calculated absorption spectrum of sample I, for the band structure of Fig. 2 with hole density of $3 \times 10^{11} \text{ cm}^{-2}$ at 80 K. Solid (dotted) line: z - (s -) polarization. (c) The p -polarized PIA spectrum of sample I, at 80 K.

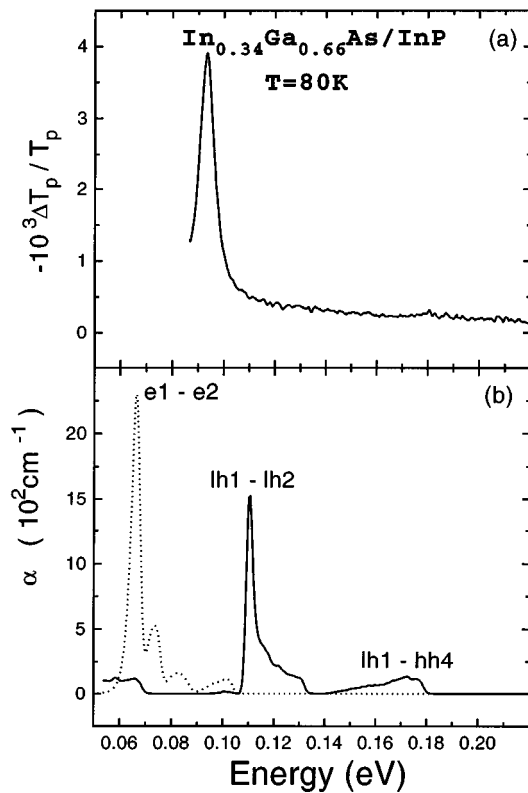


FIG. 2. (a) The PIA spectrum of sample II, at 80 K. (b) The calculated absorption spectrum of sample II, for electron-hole pairs density of $1 \times 10^{10} \text{cm}^{-2}$ at 80 K. The solid (dotted) line describes the light hole (electron) contribution.

the PIA line observed at 94 meV [Fig. 2(a)] is not due to intersubband absorption by photoexcited electrons.

Comparing the experimental results to the calculations (Table I), we see that the calculated (cal. column, Table I) lh1–lh2 transition energies (for samples I and II) are 12–14 meV higher than the observed PIA transitions (PIA column, Table I). In addition, the calculated transition for sample I is ≈ 11 meV lower than the observed absorption band (abs. column, Table I). The small discrepancy between the calculated and the observed transitions can be attributed to the uncertainty in some material constants used for the calculations.⁵ It is well known that the band offsets, valence band hydrostatic deformation potentials, and hole masses for this system are not yet very accurately determined.⁸ The difference between the transitions observed in the PIA measurement and that observed in the “dark” absorption measurement, however, deserves special attention. We note that in the *p*-doped sample (sample I), the photoinduced absorption band appears some 20 meV lower than the “dark” absorption band. This unexpected result is unlike the situation in *n*-doped InGaAs/InP⁹ and GaAs/AlGaAs¹⁰ MQWs, where the PIA band matches, in spectral position and roughly in spectral shape, the “dark” absorption. In the *n*-doped system, the “dark” absorption is due to the existing electron plasma and the PIA is due to additional electrons added to this plasma by the pump beam, thus giving rise to similar absorption bands. The existence of donor bound electrons, mainly at low temperatures, do not grossly affect this picture, since

their binding energy is relatively small (≈ 5 meV). In the present *p*-doped case, the situation is different. Here, since the binding energy of the acceptor bound holes is a few times larger than that of donor bound electrons (typically ≥ 30 meV)^{11,12} it is plausible to assume that the Be acceptors in the wells are not fully ionized even at room temperature. Certainly at 80 K, most of the “dark” absorption should be due to confined intra-acceptor transitions.

Impurity bound carriers in QWs and SLs and their effects on interband and intersubband optical transition were previously discussed by several authors. Helm *et al.*¹³ have used symmetry considerations to show that in narrow SLs, the $1s$ hydrogenic level of the donor bound electron lies a few meV lower than the first electronic subband, $e1$, while the $2p_z$ state is pinned very close in energy to the second electronic subband $e2$. The energy differences between these two states and their associated electronic bands are not the same,¹³ giving rise to slightly different $1s-2p_z$ and $e1-e2$ transition energies; the first one is always larger. We anticipate that a similar situation occurs for acceptor bound holes. Thus, intra-acceptor bound hole optical transitions in QWs are larger in energy than their associated intersubband transitions of free holes. The energy difference between the two transitions is comparable to the acceptor-hole binding energy.

We then suggest that the observed PIA is due to lh1–lh2 intersubband absorption, while the dark absorption originates from transitions between acceptor levels located close to the top of each of the lh subbands. The difference of ≈ 20 meV between the two observed bands, is the difference in binding energies between the first acceptor bound hole level (measured from lh1) and its second level (measured from lh2).

The work at the Technion was carried out in the Center for Advanced Opto-Electronics, and was partially supported by the Basic Research Foundation administered by the Israel Academy of Sciences and Humanities, Jerusalem, Israel.

¹D. Gershoni and H. Temkin, *J. Lumin.* **44**, 381 (1989).

²D. Ritter, R. A. Hamm, M. B. Panish, J. M. Vandenberg, D. Gershoni, S. D. Gunapla, and B. F. Levine, *Appl. Phys. Lett.* **59**, 552 (1991).

³M. J. Kane, M. T. Emeny, N. Aspley, C. R. Whitehouse, and D. Lee, *Semicond. Sci. Technol.* **3**, 722 (1988).

⁴D. Gershoni, J. M. Vandenberg, S.-N. G. Chu, H. Temkin, T. Tanbun-Ek, and R. A. Logan, *Phys. Rev. B* **40**, 10017 (1989).

⁵G. A. Baraff and D. Gershoni, *Phys. Rev. B* **43**, 4011 (1991); D. Gershoni, C. H. Henry and G. A. Baraff, *IEEE J. Quantum Electron.* **29**, 2433 (1993).

⁶J. Oiknine-Schlesinger, E. Ehrenfreund, D. Gershoni, D. Ritter, M. B. Panish, and R. A. Hamm, *Appl. Phys. Lett.* **59**, 970 (1991); *Solid-State Electron.* **37**, 1269 (1994).

⁷D. Gershoni, H. Temkin, J. M. Vandenberg, S.-N. G. Chu, R. A. Hamm, and B. Panish, *Phys. Rev. Lett.* **60**, 448 (1988).

⁸*Semiconductors*, edited by O. Madelung, M. Schultz, and H. Weiss, Landolt–Börnstein, New Series (Springer-Verlag, Berlin, 1982), Group 3, Vol. 17a.

⁹D. Gershoni, J. Oiknine-Schlesinger, E. Ehrenfreund, D. Ritter, R. A. Hamm, and M. B. Panish, *Phys. Rev. Lett.* **71**, 2975 (1993).

¹⁰Y. Garini, E. Ehrenfreund, E. Cohen, A. Ron, K.-K. Law, J. L. Merz, and A. C. Gossard, *Phys. Rev. B* **48**, 4456 (1993).

¹¹R. C. Miller, A. C. Gossard, W. T. Tsang, and O. Munteanu, *Phys. Rev. B* **24**, 1134 (1982).

¹²W. T. Masselink, Y.-C. Chang, and H. Morkoç, *Phys. Rev. B* **25**, 3871 (1983).

¹³M. Helm, F. M. Peeters, F. DeRosa, E. Colas, J. P. Harbison, and L. T. Florez, *Phys. Rev. B* **43**, 13983 (1991); *Phys. Rev. B* **48**, 1601 (1993).